ChemComm

COMMUNICATION

View Article Online
View Journal

Cite this: DOI: 10.1039/d6cc01502f

Received 12th March 2026,
Accepted 20th April 2026

DOI: 10.1039/d6cc01502f

rsc.li/chemcomm

Mechanochemically-synthesised AIE-active receptors for selective ceftazidime sensing in high-water-content matrices

Krzysztof Melcer, [a] Tim David, [b] Bernd M. Schmidt [b] and Artur Kasprzak *[a]

Mechanochemical synthesis of water-insoluble, AIE-active dendritic receptors enable selective fluorescence detection of ceftazidime in up to 99 vol% water. Selectivity over structurally related β-lactams was confirmed by titrations, DFT, and NMR studies. Detection remains reliable in tap water, artesian groundwater, and seawater, with a limit of detection (LOD) as low as 1.1 μM.

Mechanochemistry has emerged as a powerful non-conventional tool in modern organic synthesis, enabling sustainable synthetic protocols and access to compounds that are difficult or even inaccessible by classical in-solution methods.[1–7] Molecular receptors capable of selectively interacting with guest molecules through non-covalent interactions are highly relevant in both fundamental and applied sciences.[8–12] Among these, receptors featuring aggregation-induced emission (AIE) are particularly attractive, offering enhanced luminescence in aggregated states while simultaneously offering improved sensing performance, including sensitivity and selectivity, especially in aqueous media that remain challenging for conventional organic receptors.[13–19] Although mechanochemistry has been explored for the synthesis of AIE-active receptors,[20,21] the reported examples remain limited to a narrow set of molecular classes (such as azines,[22–25] imides,[26] and amides[27,28]) used for the detection of a limited number of analytes (such as inorganic ions,[22,27,28] hydrazine,[22,26] hydrogen peroxide,[24] and nitroaromatic compounds[23]). Nevertheless, in these studies, the advantageous properties of the receptors in the aggregated state, particularly the enhancement of detection sensitivity relative to solution-phase behaviour, have been clearly demonstrated.

Herein, we report the mechanochemical synthesis of novel dendritic amide receptors, **B3E** and **F-B3E**, composed of 1,1,2,2-tetraphenylethene (TPE) and 1,3,5-triphenylbenzene (TPB) cores, with **F-B3E** bearing twelve fluorine substituents at the TPB core (Fig. 1). Introducing fluorinated substituents into AIE luminogens enables modification of their optical properties,[29–31] with examples where up to four fluorine substituents alter absorption and emission maxima.[29,32] Both receptors exhibit strong AIE behaviour in aqueous media and selectively detect the β-lactam antibiotic ceftazidime (Cef) in aqueous solutions containing up to 99 vol% water, as established by spectrofluorimetric studies. Currently established tools allow detection of Cef with LOD values down to 0.55 nM for electrochemical sensors[33] and at the micromolar level for fluorescence-based sensors.[34–36] The performance was further validated in tap water, artesian groundwater, and seawater, establishing practical applicability for environmental antibiotic monitoring using supramolecular systems.

Preliminary attempts to synthesise the target molecules in solution and *via* sonochemistry yielded undesired mixed products. The mechanochemical approach allowed the synthesis of compounds **B3E** and **F-B3E**, giving access to dendritic-like triamides under non-conventional conditions, including the trifold coupling of the near-perfluorinated tricarboxylic acid **2**, a particularly challenging substrate, due to the electronic effect of the fluorine atoms on the reactivity of the carboxylic groups. Notably, the introduction of 12 fluorine atoms into the receptor scaffold might influence physicochemical properties, potential shifts in UV-vis absorption and fluorescence emission maxima, and a significant change of the fluorescence quantum yield. Tricarboxylic acid **1** or **2**, amine **3**, and a coupling agent, *N,N′*-dicyclohexylcarbodiimide (DCC) or carbonyldiimidazole (CDI), were ground for 4 hours with DCM (liquid-assisted grinding (LAG), η = 0.51–0.91 μL mg^{-1}) in a stainless steel (SS) jar with SS balls. Isolation of pure products required purification by column chromatography and preparative thin-layer chromatography (PTLC), yielding **B3E** and **F-B3E** in 50% and 57% yields, respectively. Notably, solution-phase amide couplings of analogous hydrogenated substrates rarely exceed 50% per side.[37]

Structure and purity were confirmed by ^{1}H NMR, $\{^{1}H\}^{13}$C NMR, ^{19}F NMR (for **F-B3E**), ^{1}H–^{1}H COSY NMR, and ESI-HRMS (for full compound characterisation data, see SI, Sections S1–S3).

[a] *Faculty of Chemistry, Warsaw University of Technology, Noakowskiego 3, 00-664 Warsaw, Poland. E-mail: artur.kasprzak@pw.edu.pl*
[b] *Institut für Organische Chemie und Makromolekulare Chemie Heinrich-Heine-Universität Düsseldorf Universitätsstraße 1, D-40225 Düsseldorf, Germany*

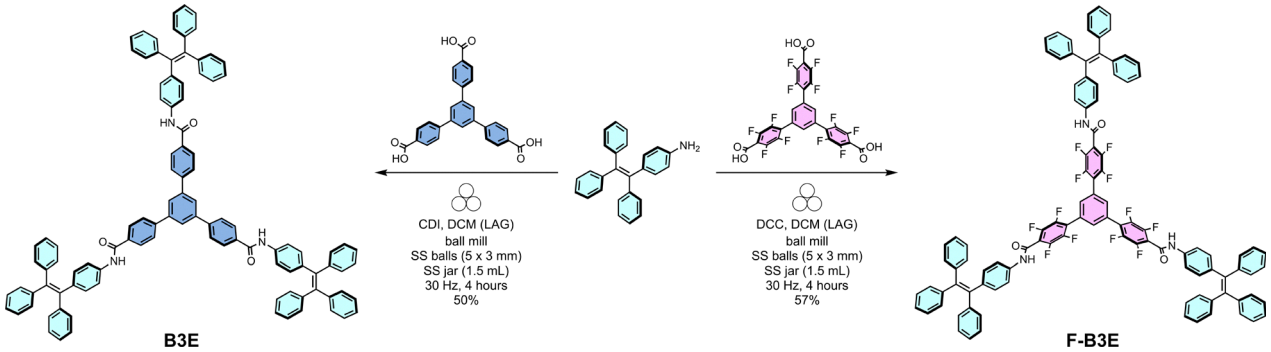

Fig. 1 Synthesis of receptors **B3E** and **F-B3E**.

The optical properties of **B3E** and **F-B3E** were studied using UV-vis and fluorescence spectroscopy. UV-vis measurements in THF solution and in the aggregated state (water : THF 95 : 5 v/v) revealed a shared solution-phase absorption maximum (λ_{max}) at 235 nm for both receptors. Upon aggregation, **B3E** showed a redshift to 261 nm accompanied by a 2-fold increase in the molar absorption coefficient (ε) value for aggregates ($\varepsilon_{solution}$ = 6.9 × 10^4 dm^3 mol^{-1} cm^{-1}, $\varepsilon_{aggregates}$ = 1.4 × 10^5 dm^3 mol^{-1} cm^{-1}). **F-B3E** shifted to 250 nm with a 10-fold decrease in ε value ($\varepsilon_{solution}$ = 2.6 × 10^5 dm^3 mol^{-1} cm^{-1}, $\varepsilon_{aggregates}$ = 2.7 × 10^4 dm^3 mol^{-1} cm^{-1}), suggesting distinct aggregation behaviour between the two receptors (SI, Section S5).

AIE behaviour was investigated by measuring fluorescence spectra in water : THF systems with increasing water content (Fig. 2; SI, Section S5.2). For **B3E**, emission onset occurred at 70% vol., with intensity rising sharply at 90% vol. and reaching a maximum at 95%. **F-B3E** showed a more gradual response, with a modest intensity increase from 60–70% vol. water content that continued to increase until 95% vol. In both cases, aggregation was accompanied by a redshift in emission maximum (λ_{em} = 480 nm and 470 nm for **B3E** and **F-B3E**, respectively, redshift range 42–84 nm). The AIE enhancement ratio (α_{AIE})[38] was 16.3 and 11.1 for **B3E** and **F-B3E**, respectively. Fluorescence quantum yield (Φ_F) was measured in dissolved and aggregated states and increased approximately 5-fold upon aggregation for both receptors Φ_F value of **B3E** (0.059) and **F-B3E** (0.109) in the aggregated state (SI, Section S5.1). The size of aggregates in different solvent systems was analysed using dynamic light scattering (DLS) (refer to SI, Section S5.3). DLS analysis revealed a 10-fold decrease in mean aggregate size with increasing water content for **B3E** and a 2.6-fold decrease for **F-B3E**. This tendency suggests a correlation between a decrease in aggregate size and an increase in fluorescence intensity, allowing to connect the process of disaggregation with a plausible mechanism of fluorescence quenching (SI, Section S5.3).

Detection of β-lactam antibiotics, which are widely used in the treatment of bacterial infections in humans, in high-water-content matrices represents a significant analytical challenge for environmental protection and monitoring.[39] Unlike conventional organic receptors, which suffer from poor aqueous solubility and aggregation-caused quenching (ACQ), AIE-active receptors inherently overcome both limitations, making **B3E** and **F-B3E** well-suited candidates for antibiotic sensing in aqueous media.

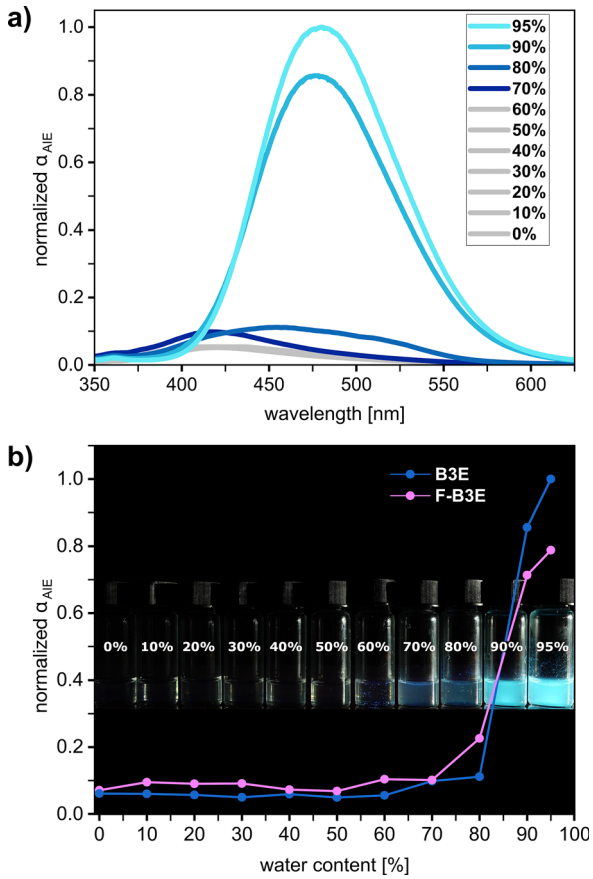

Fig. 2 (a) Relative fluorescence intensity of **B3E** a in water : THF systems with increasing water content (C = 2 × 10^{-5} M, λ_{ex} = 320 nm); (b) comparison of α_{AIE} parameter for **B3E** and **F-B3E** in THF solution and in aggregated state (water : THF 95 : 5 v : v; C = 2 × 10^{-5} M, λ_{ex} = 320 nm), inset: image of AIE effect of **B3E** in water : THF solvent systems with increasing water content (C = 2 × 10^{-5} M, λ_{ex} = 365 nm).

To assess sensing performance, spectrofluorometric titrations were conducted with **B3E** and **F-B3E** against a series of β-lactam antibiotics, namely Amoxicillin (Amox), Penicillin G (Pen), Ampicillin (Ampc), and Ceftazidime (Cef), in water : THF

(95 : 5 v/v) using ultrapure water and 0–30 equiv. of antibiotics (SI, Section S4). These antibiotics were carefully chosen due to their structural similarity and potential for binding with amide-bonding-containing molecules (refer to SI, Section S4, for structures). Both receptors responded selectively to Cef, with a 72–75% decrease in fluorescence intensity (Fig. 3a), while Pen, Ampc, and Amox produced no significant response (refer to SI, Section S6.1 for spectra). Selectivity was further confirmed by a competition experiment in which the addition of 1 equiv. Ampc did not affect the **B3E**–Cef titration curve. Analysis of the titration curves with the *Bindfit*[40,41] tool indicated a 1 : 1 stoichiometry for the Cef-receptor complexes, with association constant (K_a) values of 2.844×10^3 M^{-1} and 3.571×10^3 M^{-1} for **B3E** and **F-B3E**, respectively. Stern–Volmer constants (K_{S-V}) of 10^4 M^{-1} and limit of detection (LOD) values in the micromolar range further confirm excellent detection parameters (Table 1; see SI, Section S6.1 for spectra and plots and Section S7 for all values).

The effect of water content on receptor performance was investigated by conducting titrations at 80, 95, and 99 vol% water (SI, Section S6.1). Increasing water content to 99 vol% maintained K_{S-V} values comparable to those at 95 vol%, while delivering the lowest LOD observed across the entire study (1.1 μM for **B3E**), demonstrating effective Cef detection with minimal amount of organic solvent in the detection medium. Buffer experiments (99 : 1 buffer : THF v : v) revealed the K_{S-V} value peaked at pH = 7.4 for both receptors, with only modest differences across acidic (pH = 5.14) and basic (pH = 8.29) conditions (ΔK_{S-V} values $\leq 0.6 \times 10^3$ M^{-1}). LOD values remained in the ranges of 2.3–7.5 μM and 6.3–9.4 μM for **B3E** and **F-B3E**, respectively, across all pH conditions, with **B3E** outperforming **F-B3E** under non-neutral conditions (SI, Section S6.1 and S7).

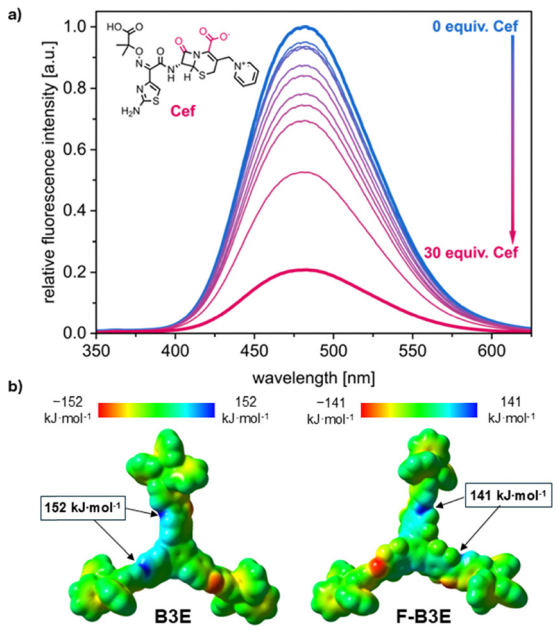

Fig. 3 (a) Fluorescence spectra of aggregated **B3E** in the presence of increasing molar equivalents of ceftazidime (Cef), conditions: water (seawater, non-filtered) : THF = 99 : 1 v/v, $C = 2 \times 10^{-5}$ mol dm^{-3}, λ_{ex} = 320 nm, inset: Cef structure with marked possible binding sites; (b) DFT-computed ESP maps of **B3E** and **F-B3E**.

Table 1 Comparison of K_{S-V}, K_a and LOD values for **B3E** and **F-B3E** in different solvent systems (water : THF = 99 : 1 v/v; full data for titrations with pure H_2O are presented in Table S10, SI)

Solvent–receptor system		$K_{s-v} \times 10^3$ [M^{-1}]	LOD [μM]
Tap water	**B3E**	3.369 ± 0.153	7.1
	F-B3E	3.159 ± 0.133	6.5
Seawater (filtered)	**B3E**	4.070 ± 0.077	2.9
	F-B3E	5.411 ± 0.228	6.5
Seawater (non-filtered)	**B3E**	4.101 ± 0.178	6.7
	F-B3E	4.346 ± 0.152	5.4
Artesian groundwater	**B3E**	4.115 ± 0.179	6.4
	F-B3E	2.423 ± 0.198	12.7

To demonstrate real-world applicability, titrations were performed in tap water, artesian groundwater (manganese-rich), and seawater (sodium-rich), with seawater tested both filtered (0.2 μm PTFE) and unfiltered (mean particle size 841 nm, polymodal distribution; SI, Section S7 for full ICP-MS characterisation). In all matrices, both receptors successfully detected Cef, with K_{S-V} and LOD values remaining comparable to those obtained in ultrapure water. **B3E** demonstrated greater robustness across environmental matrices, with K_{S-V} values showing less variation than **F-B3E** and LOD values ranging from 2.9–7.1 μM, compared to 5.4–12.7 μM for **F-B3E** (Table 1, SI S7). In addition, competitive experiments using other classes of antibiotics (tetracycline, lincosamide, rifamycin) in the form of real-world pharmaceutical products did not affect the Cef sensing, further evidencing the potential of obtained receptors (refer to SI, Section S6.1, for the full data on titrations).

DFT calculations (B3LYP[42]/6-31g(d,p)[43]) were performed to optimise the structures of **B3E** and **F-B3E** and identify potential binding sites (Fig. 3b; SI, Section S4). Both receptors feature regions of high electrostatic surface potential (ESP), centred on the amide nitrogen atoms (*ca.* 152 and 141 kJ mol^{-1} for **B3E** and **F-B3E**, respectively), with the positive potential in **B3E** more delocalised across the TPB core compared to the more localised distribution in **F-B3E**. Complementarily, ESP maps of the tested β-lactam antibiotics revealed a uniquely concentrated negative potential on the carboxylic group of Cef, which also possesses the highest number of hydrogen bond acceptors in the series (12, *versus* 5–7 for Pen, Ampc, and Amox; SI, Section S4), rationalising the observed selectivity.

^{1}H NMR titration experiments in DMSO-d_6 confirmed that the amide N–H protons of both receptors shift upon Cef addition, while aromatic proton signals remain unchanged, identifying the amide moiety as the primary binding site (SI, Section S6.2). ^{19}F NMR titration of **F-B3E** showed no fluorine signal shifts, ruling out fluorine atom participation in binding. Reverse titration (adding **B3E** to the Cef solution) produced an upfield shift of the pyridinium cation ring protons of Cef,

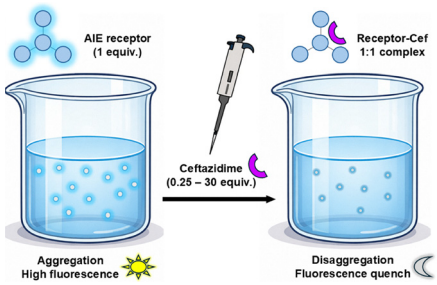

Fig. 4 Graphical representation of the detection mechanism.

consistent with receptor binding at the carboxylic group disrupting the internal ion pair. DLS measurements in the presence of 1 equiv. Cef showed a reduction in mean aggregate size of 11% and 49% for **B3E** and **F-B3E**, respectively (SI, Section S6.3), indicating that fluorescence quenching arises from a combination of direct amide–carboxylate binding and Cef-induced disaggregation (Fig. 4).

In conclusion, a mechanochemical synthesis afforded two novel AIE-active dendritic receptors, **B3E** and **F-B3E**, capable of selectively detecting ceftazidime in aqueous media containing up to 99 vol% water, enabled by their AIE properties that conventional water-insoluble receptors cannot match. Notably, introducing 12 fluorine atoms to an AIE-active molecule (**F-B3E**) led to a 2-fold increase in the fluorescence quantum yield. Detection parameters were robust across ultrapure water, buffer solutions, and real environmental matrices (tap water, artesian groundwater, and seawater), with $K_{S\text{-}V}$ and K_a at the 10^3 M^{-1} level and LOD as low as 1.1 μM. Beyond the immediate analytical application, this work establishes mechanochemical synthesis as a powerful green strategy for accessing structurally complex, functional AIE-active receptors that are difficult or inaccessible by conventional solution-phase routes. We anticipate that this approach will inspire broader exploration of mechanochemically synthesised supramolecular sensing systems, opening new avenues in sustainable materials chemistry, environmental monitoring, and the development of next-generation receptors for biorelevant analyte detection in complex aqueous matrices.

K. M. performed synthesis, characterisation and receptor experiments, analysed the data and wrote the manuscript and SI drafts with A. K. T. D. synthesised compound **1**; A. K. conceived and supervised the project, analysed the data, performed DFT studies and wrote the respective part of SI, provided funding acquisition, reviewed and edited the manuscript and supporting information drafts together with K. M., T. D. and B. M. S., as well as led the correspondence with the editor and reviewers. All authors discussed the results and commented on the manuscript.

Conflicts of interest

There are no conflicts to declare.

Data availability

The data supporting this article have been included as part of the supplementary information (SI). Supplementary information: materials and methods, experimental section, compounds characterization data, data on receptor studies, DFT calculations. See DOI: https://doi.org/10.1039/d6cc01502f.

Acknowledgements

We acknowledge support from the POB Technologie Materiałowe (CPR-IDUB/37/Z01/POB5/2024; A. K.), the National Science Centre, Poland (OPUS, 2021/43/B/ST4/00114 (A. K.), and the Warsaw University of Technology (WUT, statutory support; A. K.). This work was supported by the Jürgen Manchot Foundation (PhD fellowship to T. D.). B. M. S. acknowledges the Deutsche Forschungsgemeinschaft (DFG, German Research Foundation) SCHM 3101/6. The DFT studies were performed with support of the Interdisciplinary Centre for Mathematical and Computational Modelling University of Warsaw (ICM UW) under computational allocation no. G101-2385 (A. K.). The number of hydrogen bonding donors/acceptors for antibiotics was computed with ADMET-predictor™ (Simulations Plus, University +License).[44]

References

1 S. L. James and T. Friščić, *Chem. Soc. Rev.*, 2013, **42**, 7494.
2 J. F. Reynes, F. Leon and F. García, *ACS Org. Inorg. Au*, 2024, **4**, 432–470.
3 T. Friščić, C. Mottillo and H. M. Titi, *Angew. Chem., Int. Ed.*, 2020, **59**, 1018–1029.
4 J.-L. Do and T. Friščić, *ACS Cent. Sci.*, 2017, **3**, 13–19.
5 T. Stolar, J. Alić, L. Casali, N. Gugin, M. Baláž, A. A. L. Michalchuk and F. Emmerling, *Chem*, 2026, 102880.
6 S. L. James, C. J. Adams, C. Bolm, D. Braga, P. Collier, T. Friščić, F. Grepioni, K. D. M. Harris, G. Hyett, W. Jones, A. Krebs, J. Mack, L. Maini, A. G. Orpen, I. P. Parkin, W. C. Shearouse, J. W. Steed and D. C. Waddell, *Chem. Soc. Rev.*, 2012, **41**, 413–447.
7 T. Kunde, T. Pausch, P. A. Guńka, M. Krzyżanowski, A. Kasprzak and B. M. Schmidt, *Chem. Sci.*, 2022, **13**, 2877–2883.
8 J. H. Hartley, T. D. James and C. J. Ward, *J. Chem. Soc., Perkin Trans. 1*, 2000, 3155–3184.
9 L. Chen, S. N. Berry, X. Wu, E. N. W. Howe and P. A. Gale, *Chem*, 2020, **6**, 61–141.
10 P. A. Gale and C. Caltagirone, *Chem. Soc. Rev.*, 2015, **44**, 4212–4227.
11 K. Maslowska-Jarzyna, E. York, E. Feo, R. M. Maklad, G. Bao, M. Fares and P. A. Gale, *Chem*, 2025, **11**, 102695.
12 S. K. Kim and J. L. Sessler, *Chem. Soc. Rev.*, 2010, **39**, 3784.
13 R. T. K. Kwok, C. W. T. Leung, J. W. Y. Lam and B. Z. Tang, *Chem. Soc. Rev.*, 2015, **44**, 4228–4238.
14 F.-Y. Ye, M. Hu and Y.-S. Zheng, *Coord. Chem. Rev.*, 2023, **493**, 215328.
15 Y. Hong, J. W. Y. Lam and B. Z. Tang, *Chem. Commun.*, 2009, 4332.
16 C. Zhu, R. T. K. Kwok, J. W. Y. Lam and B. Z. Tang, *ACS Appl. Bio Mater.*, 2018, **1**, 1768–1786.
17 S. Kulczyk and A. Kasprzak, *Analysis Sensing*, 2025, e202500173.
18 M. Gao and B. Z. Tang, *ACS Sens.*, 2017, **2**, 1382–1399.
19 M. H. Chua, B. Y. K. Hui, K. L. O. Chin, Q. Zhu, X. Liu and J. Xu, *Mater. Chem. Front.*, 2023, **7**, 5561–5660.
20 J. S. Cyniak and A. Kasprzak, *ACS Omega*, 2024, **9**, 48870–48883.
21 M. Banerjee, A. A. Bhosle, A. Chatterjee and S. Saha, *J. Org. Chem.*, 2021, **86**, 13911–13923.
22 A. A. Bhosle, M. Banerjee, S. Saha, S. Garg, S. Ghosh and A. Chatterjee, *Sens. Actuators, B*, 2023, **397**, 134661.

23 A. A. Bhosle, M. Banerjee, S. D. Hiremath, A. C. Bhasikuttan and A. Chatterjee, *Chem. – Asian J.*, 2023, **18**, e202300048.
24 A. A. Bhosle, M. Banerjee, V. Gupta, S. Ghosh, A. C. Bhasikuttan and A. Chatterjee, *New J. Chem.*, 2022, **46**, 18961–18972.
25 A. A. Bhosle, S. D. Hiremath, A. C. Bhasikuttan, M. Banerjee and A. Chatterjee, *J. Photochem. Photobiol., A*, 2021, **413**, 113265.
26 S. D. Hiremath, R. U. Gawas, D. Das, V. G. Naik, A. A. Bhosle, V. P. Murali, K. K. Maiti, R. Acharya, M. Banerjee and A. Chatterjee, *RSC Adv.*, 2021, **11**, 21269–21278.
27 J. S. Cyniak and A. Kasprzak, *RSC Adv.*, 2024, **14**, 13227–13236.
28 J. S. Cyniak, K. Melcer and A. Kasprzak, *Chem. Eur. J.*, 2025, **31**, e02859.
29 A. Nitti, E. Tatsi, E. Magnani, G. Mattioli, F. Porcelli, C. Botta, G. Griffini and D. Pasini, *Chem. Commun.*, 2026, **62**, 4320–4324.
30 P. Zheng, Y. Ding, A. Abdurahman, J. Zhu, L. Tian, Y. Liu, Q. Liu, L. Wang, D. Wang and B. Z. Tang, *Sci. China: Chem.*, 2025, **68**, 3086–3099.
31 X. Lv, Y. Bao, H. Zhou and Y. Qu, *Dyes Pigm.*, 2025, **233**, 112525.
32 H. Zhang, Y. Nie, J. Miao, D. Zhang, Y. Li, G. Liu, G. Sun and X. Jiang, *J. Mater. Chem. C*, 2019, **7**, 3306–3314.
33 M. Torkashvand, M. B. Gholivand and G. Malekzadeh, *Sens. Actuators, B*, 2016, **231**, 759–767.
34 J. Hu, Y. Ma and S. Wu, *Spectrochim. Acta, Part A*, 2025, **327**, 125341.
35 S. Fathi, *Russ. J. Electrochem.*, 2014, **50**, 468–475.
36 A. de, H. Moreno and H. R. N. Salgado, *J. AOAC Int.*, 2009, **92**, 820–823.
37 L. Zhang, S. Jiang, Z. Yi, M. Peng, F. Wang and Y. Tian, *Chem. Commun.*, 2026, **62**, 3526–3530.
38 R. Hu, N. L. C. Leung and B. Z. Tang, *Chem. Soc. Rev.*, 2014, **43**, 4494–4562.
39 K. M. Sta Ana, J. Madriaga and M. P. Espino, *Environ. Pollut.*, 2021, **275**, 116624.
40 D. Brynn Hibbert and P. Thordarson, *Chem. Commun.*, 2016, **52**, 12792–12805.
41 P. Thordarson, *Chem. Soc. Rev.*, 2011, **40**, 1305–1323.
42 A. D. Becke, *J. Chem. Phys.*, 1993, **98**, 5648–5652.
43 J. S. Binkley, J. A. Pople and W. J. Hehre, *J. Am. Chem. Soc.*, 1980, **102**, 939–947.
44 ADMET Predictor, https://www.simulations-plus.com.